0026-895X/03/6402-235–248$7.00
MOLECULAR PHARMACOLOGY
Copyright © 2003 The American Society for Pharmacology and Experimental Therapeutics
Mol Pharmacol 64:235–248, 2003

Vol. 64, No. 2
2568/1082501
Printed in U.S.A.

Key Roles of Phe^{1112} and Ser^{1115} in the Pore-Forming IIIS5-S6 Linker of L-Type Ca^{2+} Channel α_{1C} Subunit ($Ca_V1.2$) in Binding of Dihydropyridines and Action of Ca^{2+} Channel Agonists

SHINJI YAMAGUCHI, BORIS S. ZHOROV, KATSURO YOSHIOKA, TAKU NAGAO, HIDENORI ICHIJO, and SATOMI ADACHI-AKAHANE

Laboratory of Cell Signaling, Graduate School of Pharmaceutical Sciences, the University of Tokyo, Tokyo, Japan (S.Y., K.Y., H.I., S.A.-A.); Department of Biochemistry, McMaster University, Hamilton, Ontario, Canada (B.S.Z.); and National Institute of Health Sciences, Kamiyoga, Setagaya-ku, Tokyo, Japan (T.N.)

Received April 7, 2003; accepted April 28, 2003

This article is available online at http://molpharm.aspetjournals.org

ABSTRACT

Voltage-dependent L-type Ca^{2+} channels are modulated by the binding of Ca^{2+} channel antagonists and agonists to the pore-forming α_{1C} subunit ($Ca_V1.2$). We recently identified Ser^{1115} in IIIS5-S6 linker of α_{1C} subunit as a critical determinant of the action of 1,4-dihydropyridine agonists. In this study, we applied alanine-scanning mutational analysis in IIIS5-S6 linker of rat brain α_{1C} subunit (rbCII) to illustrate the role of pore-forming IIIS5-S6 linker in the action of Ca^{2+} channel modulators. Ca^{2+} channel currents through wild-type (rbCII) or mutated α_{1C} subunits, transiently expressed in BHK6 cells with β_{1a} and α_2/δ subunits, were analyzed. The replacement of Phe^{1112} by Ala (F1112A) significantly impaired the sensitivity to Ca^{2+} channel agonists (*S*)-(−)-Bay k 8644 and FPL-64176, and modestly to 1,4-dihydropyridine (DHP) antagonists. The low sensitivity of F1112A and S1115A to DHP antagonists was consistent with the reduced binding affinity for [^{3}H](+)PN200-110. The replacement of Phe^{1112} by Tyr, but not by Ala, restored the long openings produced by FPL-64176, thus indicating the critical role of aromatic ring of Phe^{1112} in the Ca^{2+} channel agonist action. Interestingly, double-mutant Ca^{2+} channel (F1112A/S1115A) failed to discriminate between Ca^{2+} channel agonist (*S*)-(−)-1,4-dihydro-2,6-dimethyl-5-nitro-4-(2-[trifluoromethyl] phenyl)-3-pyridine carboxylic acid methyl ester (Bay k 8644) and antagonist (*R*)-(+)-Bay k 8644 and was blocked by the two enantiomers in an identical manner. These results indicate that both Phe^{1112} and Ser^{1115} in linker IIIS5-S6 are required for the action of Ca^{2+} channel agonists. A model of the DHP receptor is proposed to visualize possible interactions of Phe^{1112}, Ser^{1115}, and other DHP-sensing residues with a typical DHP ligand nifedipine.

Voltage-dependent L-type Ca^{2+} channels play critical roles in shaping action potentials, excitation-contraction coupling, excitation-secretion coupling, and gene expression. L-type Ca^{2+} channel currents are blocked by classic Ca^{2+} channel antagonists such as 1,4-dihydropyridines (DHP), benzothiazepines (BTZ), and phenylalkylamines (PAA) (Regulla et al., 1991; Striessnig et al., 1998), whereas other non–L-type Ca^{2+} channel currents are less sensitive to Ca^{2+} channel antagonists. Ca^{2+} channel agonists such as DHP compounds and a benzoylpyrrole derivative, FPL-64176, enhance L-type Ca^{2+} channel currents through prolongation of the channel open time and enhancement of the open probability (Zheng et al., 1991; Adachi-Akahane and Nagao, 2000). DHP Ca^{2+} channel agonists have been shown to exert antagonistic effects at high concentrations (Usowicz et al., 1995) or at depolarized membrane potentials. In contrast, FPL-64176 binds to the Ca^{2+} channel at the binding site distinct from that of DHPs (Rampe and Lacerda, 1991), and produces exclusively Ca^{2+} channel agonistic action even at very high concentrations without Ca^{2+} channel antagonistic effects.

Critical determinants of the high-affinity binding sites for Ca^{2+} channel antagonists and agonists on L-type Ca^{2+} channel have been identified. However, conformational changes of the Ca^{2+} channel during modulation by these compounds and the molecular mechanism underlying the differences between Ca^{2+} channel agonists and antagonists are largely unknown. The elucidation of DHP binding pocket is espe-

This work was supported by a Grant-in-Aid for Scientific Research from the Japanese Society for the Promotion of Science and by a grant to BSZ from the Canadian Institutes of Health Research (CIHR). B.S.Z. is a recipient of the CIHR Senior Scientist award.

This work is part of the Ph.D. thesis of S.Y.

This work was presented in part as an abstract [Yamaguchi S and Adachi-Akahane S (2002) Role of the IIIS5-S6 linker of L-type Ca^{2+} channel α_{1C} subunit in the action of Ca^{2+} channel agonist. *Biophys J* **82:**103A].

ABBREVIATIONS: DHP, dihydropyridine; BTZ, benzothiazepine; PAA, phenylalkylamine; Bay k 8644, 1,4-dihydro-2,6-dimethyl-5-nitro-4-(2-[trifluoromethyl] phenyl)-3-pyridine carboxylic acid methyl ester; FPL-64176,2,5-dimethyl-4-[2- (phenylmethyl) benzoyl]-1H-pyrrole-3-carboxylic acid methyl ester; rbCII, rat brain Ca^{2+} channel α_{1C} subunit type II; GFP, green fluorescence protein; I-V, current-voltage.

cially important because only DHP derivatives have both Ca^{2+} channel agonists and antagonists, whereas neither BTZ nor PAA agonists are known. Amino acid residues involved in the binding pocket of DHP agonists and antagonists have been determined (Fig. 1B) (Grabner et al., 1996; Mitterdorfer et al., 1996; Peterson et al., 1996; Schuster et al., 1996; He et al., 1997; Wappl et al., 2001). The previous studies have mostly depended on differences in amino acid residues between DHP-sensitive α_{1C} subunit and DHP-insensitive subunit such as α_{1A} and α_{1E}. Considering that $\alpha_{1A\text{-}DHP}$ (Hockerman et al., 1997; Sinnegger et al., 1997) has completely gained the sensitivity to DHPs by transferring nine amino acids, the DHP binding pocket may involve unidentified amino acid residues common between α_{1A} subunit and α_{1C} subunit. Indeed, some amino acids involved in the binding pocket turned out to be conserved in DHP-insensitive α_1 subunits (Peterson et al., 1997).

We recently identified Ser^{1115}, located between IIIS5 and IIIS6 of the pore-forming α_1 subunit of L-type Ca^{2+} channel, as a critical determinant of the action of DHP agonists (Yamaguchi et al., 2000). The facts that high-affinity DHP-binding was stabilized by the binding of Ca^{2+} to the Ca^{2+} channel pore (Glossmann and Striessnig, 1990; Peterson and Catterall, 1995; Striessnig et al., 1998) and that IIIS5-S6 linker was photoaffinity labeled by photoreactive DHPs (Striessnig et al., 1991) also support the idea that DHPs interact with the pore-forming region of the Ca^{2+} channel. In the present study, we aimed at clarifying the role of the pore-forming region of α_{1C} subunit in the modulation of gating kinetics by Ca^{2+} channel agonists. For this purpose, we applied alanine-scanning mutational analysis in IIIS5-S6 linker of rat brain Ca^{2+} channel α_{1C} subunit (rbCII, $Ca_v1.2$).

We found that Phe^{1112} contributes to the binding pockets for DHPs along with Ser^{1115} in IIIS5-S6 linker and that both Phe^{1112} and Ser^{1115} are required for transducing the binding of Ca^{2+} channel agonists into the Ca^{2+} channel agonistic action.

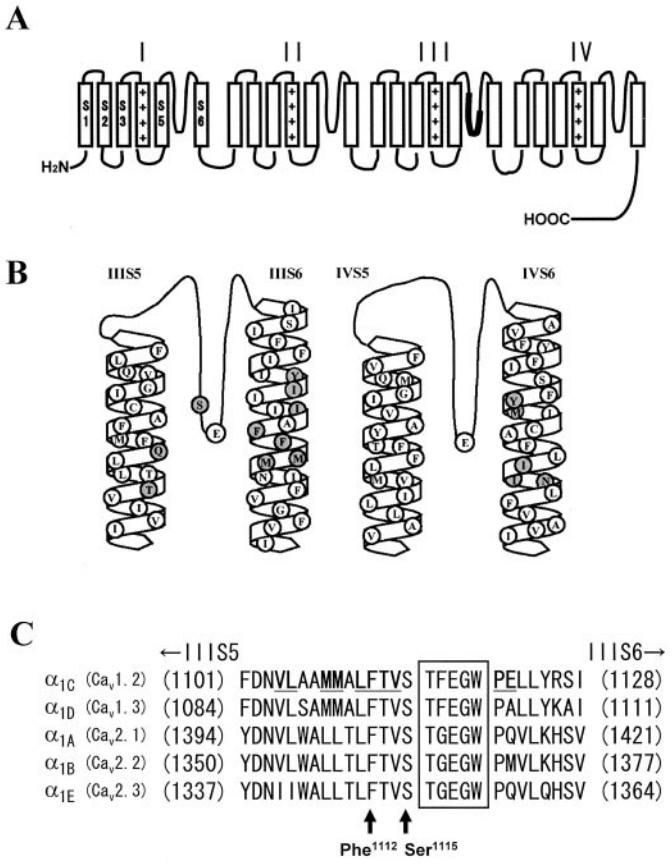

Fig. 1. Schematic drawing of DHP agonists and antagonists interaction domains of rat brain L-type Ca^{2+} channel α_{1C} subunit ($Ca_v1.2$). A, schematic drawing of Ca^{2+} channel α_{1C} subunit. Site-directed mutagenesis was introduced into the region shown in a thick line. B, schematic drawing of DHP Ca^{2+} channel agonists and antagonists interaction domains. The putative pore region in IIIS5–IIIS6 and IVS5–IVS6 of α_{1C} subunit are shown. Amino acid residues shown in gray circles have been determined as critical amino acids for the interaction with DHPs. Binding of Ca^{2+} ion to glutamic acids in the selective filter indicated in each S5-S6 linker also contributes to the affinity of DHP binding. C, sequence alignment of the pore-forming region of α_1 subunits. Sequence alignments of IIIS5-IIIS6 linker of Ca^{2+} channel α_1 subunits are shown: α_{1A} ($Ca_v2.1$), rat brain Ca^{2+} channel α_{1A} subunit (accession number M64373); α_{1B} ($Ca_v2.2$), rat brain Ca^{2+} channel α_{1B} subunit (accession number M92905); α_{1C} ($Ca_v1.2$), rat brain Ca^{2+} channel α_{1C} subunit (rbCII; accession number M67515); α_{1D} ($Ca_v1.3$), homo sapiens neuronal Ca^{2+} channel α_{1D} subunit (accession number M76558); α_{1E} ($Ca_v2.3$), rat brain Ca^{2+} channel α_{1E} subunit (GenBank accession number AY029412). Amino acids that were replaced by alanine in this experiment are underlined. Highly conserved region around the Ca^{2+} selective filter, glutamic acids, is boxed.

Materials and Methods

Point Mutations. Alanine-scanning mutagenesis was performed in 10 amino acids in IIIS5-S6 linker of rat brain α_{1C} subunit (rbCII) that was kindly supplied by Dr. T. P. Snutch (Snutch et al., 1991) using QuikChange method (QIAGEN) (Fig. 1, A and C). Single point mutations in IIIS5-S6 linker were introduced into *Pst*I (3384) to *Xmn*I (3743) fragment of rbCII as described previously (Yamaguchi et al., 2000). Polymerase chain reaction was performed using *Pfu*-turbo polymerase (Stratagene, La Jolla, CA) and verified by sequence analysis.

Single point mutations of F357A, F700A, and F1413A were introduced into rbCII (full length). Polymerase chain reaction was performed using *Pfu*-turbo polymerase (Stratagene). After polymerase chain reaction, *Bam*HI (1193) to *Bam*HI (1434) region (F357A), *Bsp*1407I (1984) to *Spe*I (3090) region (F700A), and *Bsp*HI (3736) to *Eco*RV (4515) region (F1413A) of PCR products were verified by sequence analysis and introduced into the respective region of rbCII. All α_{1C} mutants were inserted into the expression plasmid pcDNAIII.

Cell Culture and Transfection. Mutated α_{1C} subunits and rbCII were transiently expressed in BHK6 cells that stably express rabbit β_{1a} and α_2/δ subunits (Wakamori et al., 1998) as described previously (Yamaguchi et al., 2000). For electrophysiological experiments, α_{1C} mutants in pcDNAIII were transfected together with GFP (pEGFPC2) using Superfect (Qiagen). Cells were used for experiments 24~48 h after transfection. For DHP binding assay, α_{1C} mutants in pcDNAIII were transfected using LipofectAMINE Plus (Invitrogen) and membranes were prepared 48 h after transfection.

Whole-Cell Patch-Clamp Recording. The whole-cell L-type Ca^{2+} channel currents were recorded with Ca^{2+} (2 mM) or Ba^{2+} (2 mM; Fig. 6B) as a charge carrier in bath solution containing 137 mM NaCl, 5.4 mM KCl, 1 mM $MgCl_2$, 10 mM glucose, 10 mM HEPES, and 2 mM $CaCl_2$ or $BaCl_2$, pH adjusted to 7.4 with NaOH, at room temperature as described previously (Yamaguchi et al., 2000). The resistance of the heat-polished patch pipettes ranged between 2 and 4 MΩ when filled with the internal solution composed of 120 mM CsCl, 20 mM TEACl, 14 mM EGTA, 5 mM MgATP, 5 mM Na_2 creatine phosphate, 0.2 mM GTP, 10 mM HEPES, and 0.2 mM cAMP, pH adjusted to 7.3 with CsOH. Whole-cell currents were measured using a patch/whole-cell clamp amplifier (NIHON KOHDEN, Tokyo, Japan) via analog-to-digital con-

verter (Digidata 1200; Axon Instruments Inc., Union City, CA). Voltage-clamp protocols and data acquisitions were performed using pCLAMP6 software (Axon Instruments, Inc., Union City, CA).

Single-Channel Recording. Cell-attached single-channel recordings were performed with a high-K^+ bath solution (5 mM KCl, 112 mM potassium aspartate, 5 mM NaCl, 3 mM $MgCl_2$, 1 mM Mg-ATP, 2 mM EGTA, 10 mM glucose, 10 mM HEPES, pH adjusted to 7.3 with KOH, at room temperature) to cancel membrane potential. The resistance of the Cylgard 184 (Dow Corning, Midland, MI)-coated, heat-polished microelectrodes was between 6 and 10 MΩ when filled with the internal solution composed of 110 mM $BaCl_2$ and 10 mM HEPES, pH adjusted to 7.4 with TEAOH. Single-channel currents were measured using an Axopatch 200B (Axon Instruments) via analog-to-digital converter (Digidata 1200; Axon Instruments). Voltage-clamp protocols, data acquisitions, and analysis of data were performed using pCLAMP7 software (Axon Instruments).

Radioligand Binding. Cell membranes were prepared for DHP binding assay from BHK6 cells. Transfected BHK6 cells were washed two times, scraped, and homogenized using a glass-Teflon homogenizer in binding buffer (50 mM Tris, 1 mM EDTA, 100 mM phenylmethylsulfonyl fluoride, 2 mg/ml aprotinin, 100 mM benzamidine, 1 mM pepstatin A, and 1 mg/ml leupeptin, pH 7.5). The homogenate was centrifuged at 700*g* for 5 min. The pellet was rehomogenized and centrifuged again. The collected supernatants were centrifuged at 100,000*g* for 30 min. After removing the supernatant, pellet was homogenized in small volume of binding buffer, frozen in liquid nitrogen, and stored at −70°C until use. Radioligand binding studies were carried out as described previously (Ikeda et al., 1994). Membranes of BHK6 cells (approximately 0.2 mg of protein/ml) were incubated with 0.1 to 2.5 nM [^{3}H](+)-PN200-110 in a total volume (0.2 ml) of 50 mM Tris-HCl, pH 7.5, containing 1.25 mM $CaCl_2$ and 1.25 mM $MgCl_2$. In the experiments with S1115A, 2.5 to 62.5 nM [^{3}H](+)-PN200-110 was used.

The dissociation constant (K_d) and the receptor density (B_{max}) were estimated by fitting the saturation curve to the equation $[B] = (B_{max} \times F)/(K_d + F)$, where B is the ligand-receptor complex and F is concentration of ligand. The nonspecific binding was measured in the presence of 10 μM nicardipine and subtracted from the total binding to obtain the specific binding. A high ratio of specific to nonspecific binding of 0.1 to 2.5 nM [^{3}H](+)PN200-110 was observed in binding experiments with rbCII and F1112A (69~98%).

Modeling the Pore Region of rbCII. The X-ray structure of the KcsA K^+ channel (Doyle et al., 1998) was used to build the homology model of the pore region of rbCII. The model involves eight transmembrane segments, S5, S6, and four P-loops (Table 1), which are not linked to each other. Analogous segments of KcsA and rbCII are aligned as shown in Table 1. The DHP receptor model (Zhorov et al., 2001) was taken as the starting approximation for building the rbCII model. The energy of the model was optimized using the Monte Carlo-minimization method as described previously (Zhorov et al., 2001).

In describing the KcsA-based three-dimensional model of rbCII, we use a general scheme of labeling residues in ion channels (Zhorov et al., 2001). In this scheme, residues that correspond to the beginning of transmembrane helices in KcsA are assigned number 1 with a prefix indicating the repeat number and segment name. For example, Thr^{1038} of rbCII is designated $Thr^{IIIS5.14}$ because it is located in segment IIIS5 and aligns with 14th residue in M1 of KcsA (Table 1). In P-loops, selectivity-filter glutamates, which are the most conserved residues in Ca^{2+} channels, are assigned number 50. This marker is used to count residues in the aligned sequences. For example, Phe^{1112} and Ser^{1115} of rbCII are designated $Phe^{IIIP.44}$ and $Ser^{IIIP.47}$, respectively (Table 1). In some cases, residues are designated with both their genuine number and general label [e.g., $Thr^{1038(IIIS5.14)}$].

Materials. Diltiazem (generous gift from Tanabe Seiyaku) and verapamil (purchased from Nacalai Tesque, Kyoto, Japan) were dissolved in distilled water and stored at 4°C as 1 mM stock solutions. Nitrendipine (purchased from Funakoshi Seiyaku, Tokyo, Japan), (*S*)-(−)-Bay k 8644, (*R*)-(+)-Bay k 8644, and FPL-64176 (purchased from Sigma Chemical, St. Louis, MO) were dissolved in ethanol and stored at −20°C as 3 or 30 mM stock solutions. Drugs were dissolved in the external solution and applied via concentration-clamp apparatus (Vibraspec, Inc., Philadelphia, PA) in the whole-cell, patch-clamp recording. The concentration-clamp apparatus allowed us to exchange the extracellular solution within 50 ms (Adachi-Akahane et al., 1996).

[^{3}H](+)PN200-110 (82.0 Ci/mmol) was purchased from Amersham Biosciences (Little Chalfont, Buckinghamshire, UK). Nicardipine (purchased from Sigma Chemical) was dissolved in ethanol and stored at −20°C.

Statistical Analysis. Data are expressed as the mean ± S.E.M. Statistical significance was assessed with Student-Welch's *t* test or Dunnett's test and considered significant when the *p* value was less than 0.05.

TABLE 1

Aligned sequences of KcsA and rbCII

Segment M1 in KcsA is aligned with segments S5 in Ca^{2+} channels as proposed by Huber et al. (2000). The alignment of segment M2 in KcsA with segments S6 and in Ca^{2+} channels, as well as alignment of P-loops between KcsA and Ca^{2+} channels, were proposed by Zhorov et al. (2001). Residues whose mutations are known to affect binding of DHPs in L-type calcium channels, as well as two putative DHP-binding residues studied in this work, are underlined. M2 residues that face the pore in the X-ray structure of KcsA are bold.

Channel	Segment	No of First Residues	Sequence		
			1[a]	11	21
KcsA	M1	23	ALHWRAAGAA	TVLLVIVLLA	GSYLAVLAE
RbCII	IS5	262	IKAMVPLLHI	ALLVLFVIII	YAIIGLELF
	IIS5	645	LNSVRSIASL	LLLLFLFIII	FSLLGMQLF
	IIIS5	1026	FVAIRTIGNI	VIVTTLLQFM	FACIGVQLF
	IVS5	1357	IKSFQALPYV	ALLIVMLFFI	YAVIGMQVF
			33[b]	41	51
KcsA	P	59	LITYPRAL	WWSVETATTV	GYGDLYPVT
RbCII	IP	346	FDNFAFAM	LTVFQCITME	GWTDVLYWM
	IIP	689	FDNFPQSL	LTVFQILTGE	DWNSVMYDG
	IIIP	1101	FDNVLAAM	MALFTVSTFE	GWPELLYRS
	IVP	1402	FQTFPQAV	LLLFRCATGE	AWQDIMLAC
			1[a]	11	21
KcsA[b]	M2	86	LWGRCV**AV**VV	**MV**AG**I**TS**FG**L	VT**A**ALATWFV
RbCII	IS6	379	ELPWVYFVSL	VIFGSFFVLN	LVLGVLSGEF
	IIS6	727	MLVCIYFIIL	FICGNYILLN	VFLAIAVDNL
	IIIS6	1143	VEISIFFIIY	IIIIAFFMMN	IFVGFVIVTF
	IVS6	1453	SFAVFYFISF	YMLCAFLIIN	LFVAVIMDNF

[a] Numbers relative to the first residue in the corresponding α-helix of KcsA structure (Doyle et al., 1998).
[b] Numbers relative to the selectivity-filter glutamate, for which number 50 is assigned.

Results

Alanine Scanning Mutagenesis of IIIS5-S6 Linker. We have previously determined $Ser^{1115(IIIP47)}$, located in the pore-forming region of the L-type Ca^{2+} channel α_{1C} subunit (rbCII; Fig. 1, B and C) (Snutch et al., 1991), as a novel determinant of the interaction with DHPs and Ca^{2+} agonists (Fig. 1B) (Yamaguchi et al., 2000). $Ser^{1115(IIIP47)}$ is located in the N-terminal part of the P-loop. In bacterial K^+ channel KcsA, an analogous part of the P-loop forms an α-helix called the pore helix (Doyle et al., 1998). We therefore examined whether amino acid residues in the pore-forming region other than Ser^{1115} might contribute to the DHP-action. To search for amino acid residues involved in the action of Ca^{2+} channel agonists, we employed alanine-scanning mutagenesis in IIIS5-S6 linker (Fig. 1, A and C). Alanine scanning was chosen for this experiment for the following reasons: 1) the N terminus of P-loop was modeled as an α-helix (Lipkind and Fozzard, 2001; Zhorov et al., 2001) and 2) substitution of Ala in the α-helix is expected to remove the amino acid side chain in each position without causing global conformational changes (Blaber et al., 1993; Peterson et al., 1997). Most of the amino acid residues around $Ser^{1115(IIIP47)}$, except for original alanine residues ($Ala^{1106(IIIP38)}$, $Ala^{1107(IIIP39)}$, and $Ala^{1110(IIIP.42)}$), were systematically replaced by alanine (Fig. 1C). Amino acid residues just around $Glu^{1118(IIIP50)}$ (Fig. 1C, black box), which is supposed to serve as a Ca^{2+}-selective filter (Tang et al., 1993), were not replaced because their influence on Ca^{2+} channel kinetics is too large (Williamson and Sather, 1999). Among the alanine-substituted mutant Ca^{2+} channels, L1111A channel turned out to be nonconducting. The responsiveness of mutant Ca^{2+} channels to Ca^{2+} channel agonists were screened as a relative increase of Ca^{2+} channel currents by Ca^{2+} agonist FPL-64176.

FPL-64176 dramatically altered the gating kinetics of Ca^{2+} channel currents of rbCII and most of the mutants as has been reported (Fig. 2) (Zheng et al., 1991; Kunze and Rampe, 1992). 1) peak Ca^{2+} channel currents were augmented; 2) tail current duration was prolonged; 3) both activation and inactivation kinetics of Ca^{2+} channel currents were slowed down (Fig. 2A). In contrast, FPL-64176 exerted its effects on F1112A channel currents to significantly smaller extent (Fig. 2, A and B). Because effects of Ca^{2+} agonists depend on test potentials, actions of FPL-64176 on I-V relationships of F1112A channels were examined as shown in Fig. 2C. Agonistic effects of FPL-64176 on F1112A were weaker at all test voltages compared with those on rbCII (Fig. 2C), indicating that F1112A either has low binding affinity for FPL-64176 or lacks the component necessary for agonistic action. Interestingly, when $Thr^{1113(IIIP45)}$ (adjacent to $Phe^{1112(IIIP44)}$) was replaced by Ala (T1113A), the effect of FPL-64176 (1 μM) was significantly reinforced (Fig. 2, A and B). The enhanced response to FPL-64176 in T1113A was not caused by the change of the voltage-dependence of activation because its I-V relationships were not altered (data not shown). The rest of mutant Ca^{2+} channels were enhanced by FPL-64176 to the same extent as that of rbCII.

Influence on the Action of Ca^{2+} Agonists of the Replacement of Phe in Each S5-S6 Linker of Repeats I~IV. $Phe^{1112(IIIP44)}$ is six amino acids upstream from the selective filter $Glu^{1118(IIIP50)}$ (Figs. 1C and 3A) in the IIIS5-S6 linker. Multiple sequence alignment of different α_1 subunits shows that sequence motif '- -F- - -T-E-W- -' is highly conserved among Ca^{2+} channels (Fig. 1C). Furthermore, this motif is also highly conserved among the four repeats (I~IV) (Fig. 3A). Therefore, we examined the contribution of each Phe to the action of FPL-64176 by comparing mutants F357A, F700A, F1112A, and F1413A. Among the four conserved Phe residues, $Phe^{1112(IIIP44)}$, but not $Phe^{357(IP44)}$, $Phe^{700(IIP44)}$, or $Phe^{1413(IVP44)}$, turned out to be responsible for the action of FPL-64176 (Fig. 3B).

Contribution of Phe^{1112} to Pharmacological Properties of the Ca^{2+} Channel. Ca^{2+} channel currents of F1112A were slightly enhanced by the DHP agonist (*S*)-(−)-Bay k 8644, but the increment was significantly smaller than that of rbCII (Fig. 3). These results indicate that F1112A is practically insensitive to Ca^{2+} channel agonists.

Next, we examined effects of the DHP antagonist nitrendipine on F1112A and rbCII. F1112A was significantly less sensitive to nitrendipine than rbCII (Table 2). The low sensitivity to nitrendipine was estimated by the shift of the concentration-response curve. Nitrendipine blocked rbCII and mutant Ca^{2+} channels in a concentration-dependent manner. As summarized in Table 2, IC_{50} values for the block of F1112A and S1115A by nitrendipine measured at the holding potential of −70 mV were, respectively, 5.13 and 39.4 times higher than that of rbCII. When the holding potential was depolarized from −70 to −50 mV, the block of F1112A channel by nitrendipine was enhanced. However, it was still significantly weaker than that of rbCII (data not shown). On the other hand, the block of Ca^{2+} channel currents through F1112A by diltiazem or verapamil was identical to that of rbCII (Fig. 5, B and D). These results indicate that Phe^{1112} contributes to the sensitivity of rbCII to Ca^{2+} channel agonists and DHP but not to BTZ or PAA.

Because changes of electrophysiological properties of Ca^{2+} channels by mutation may affect pharmacological properties, we analyzed kinetics of F1112A channel currents (Fig. 6). The I-V curves were not different between rbCII and F1112A (Fig. 6A). Steady state inactivation curve of F1112A was shifted to the positive voltages compared with that of rbCII (-31.8 ± 1.3 versus -36.7 ± 0.53 mV, $p < 0.05$; Fig. 6B). The restitution curves and recovery time constants were not significantly different between rbCII and F1112A (Fig. 6C). Because Ca^{2+} channel antagonists preferentially bind to the Ca^{2+} channel in the inactivated state, the effects of Ca^{2+} channel antagonists may be altered by mutations as a consequence of the alteration of gating properties of the Ca^{2+} channel, such as activation and inactivation. However, at −70 mV, the fraction of the inactivated channel was indistinguishable for the mutant and rbCII. Therefore, it is unlikely that the changes in the steady-state inactivation curve account for the observed loss of DHP sensitivity in F1112A. This was supported by the results that the sensitivity to block by non-DHP Ca^{2+} channel antagonists was not altered by mutations (Fig. 5). These results indicate that the selective impairment in F1112A of the sensitivity to Ca^{2+} channel agonists and DHPs were not caused by the alteration of gating properties.

Reduced Binding Affinity to DHP Antagonist [^{3}H](+)PN200-110 of Mutant Ca^{2+} Channels. To clarify whether F1112A has low binding affinity for DHPs or has low efficacy for DHP action, we compared the sensitivity of mutant Ca^{2+} channels with that of DHP antagonist (IC_{50} val-

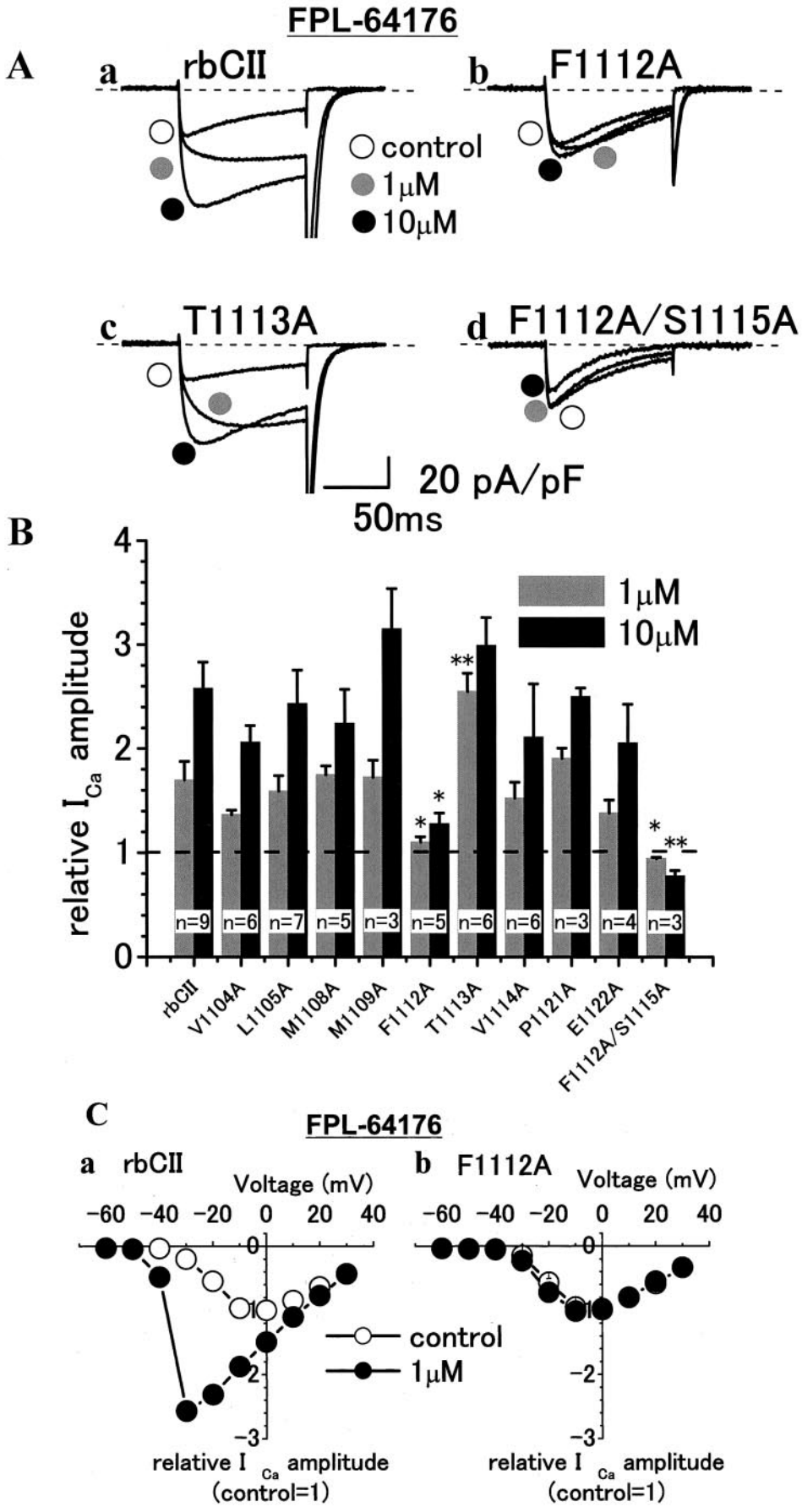

Fig. 2. Effects of FPL-64176 (1 and 10 μM) on Ca^{2+} channel currents. A, representative current traces of rbCII (a), F1112A (b), T1113A (c), and F1112A/S1115A (d) with and without FPL-64176 elicited by test pulses to 0 mV for 100 ms from a holding potential of −70 mV applied at 0.1 Hz. ○, control Ca^{2+} channel currents. Other circles represent Ca^{2+} channel currents recorded in the presence of FPL-64176 at 1 (◍) and 10 μM (●). In F1112A channel, enhancement of peak Ca^{2+} channel currents and the prolongation of tail currents were significantly weak. Ca^{2+} channel currents through F1112A/S1115A were blocked by FPL-64176 in a concentration-dependent manner. B, summary of relative change by FPL-64176 of peak Ca^{2+} channel currents through IIIS5-S6 mutants. Horizontal dashed line indicates the control Ca^{2+} channel current level. *, $p < 0.05$ versus rbCII. **, $p < 0.01$ versus rbCII. Error bars show S.E.M. C, effects of FPL-64176 (1 μM) on I-V relationships of rbCII (a) and F1112A (b). Regardless of test voltages, effects of FPL-64176 on F1112A channel currents were weaker than that of rbCII.

ues, Table 2) and the binding affinity of mutant Ca^{2+} channels to DHP antagonist estimated by radioligand binding assay (Table 3). The K_d values for [^{3}H](+)PN200-110 binding of rbCII and mutant Ca^{2+} channels were estimated by the saturation curve of specific binding. K_d and B_{max} of the [^{3}H](+)PN200-110 binding to Ca^{2+} channels are summarized in Table 3. The relative change of K_d values was consistent with that of IC_{50} values, thus indicating that the reduced sensitivity of F1112A and S1115A to DHP antagonists resulted from the reduced binding affinity. The IC_{50} values measured at a holding potential of −70 mV was higher by 1,000~3,000-fold than K_d values measured in membrane fractions where membrane potential was supposed to be near 0 mV (Table 2, 3). These results are explained by the voltage-dependence of the binding affinity of DHPs to Ca^{2+} channels (Bean, 1984).

Effects of FPL-64176 on Unitary Ca^{2+} Channel Currents of rbCII and F1112A. Considering that the decay rate of whole-cell Ca^{2+} channel currents of F1112A was not slowed by FPL-64176 (Fig. 2A, b), insensitivity of F1112A to Ca^{2+} channel agonists may be caused by the lack of ability to prolong mean open time. In the presence of FPL-64176, rbCII showed unitary Ca^{2+} channel currents with long openings (Fig. 7A). However, F1112A currents showed only short openings even in the presence of FPL-64176 at high concentrations (30 μM). In F1112A, Ca^{2+} channel agonist increased the open probability, but there was little enhancement of the mean open time (Fig. 7B).

Pharmacological Properties of Double Mutant Ca^{2+} Channel F1112A/S1115A. We have previously shown that S1115A was also less sensitive to DHP agonists and antagonists (Yamaguchi et al., 2000). Accordingly, we studied whether the mutational influences of the two amino acid residues are additive. The ratio of the IC_{50} value of F1112A/S1115A versus S1115A and F1112A/S1115A versus F1112A were 1.27 and 9.79, respectively (Table 2), suggesting that Ser^{1115} exerts larger contribution to the sensitivity to DHP than Phe^{1112} and that their influences are not additive.

Interestingly, effects of Ca^{2+} channel agonists were quite different between S1115A and F1112A/S1115A. (*S*)-(−)-Bay k 8644 as well as FPL-64176 decreased Ca^{2+} channel currents through F1112A/S1115A (Figs. 2B and 4). Therefore,

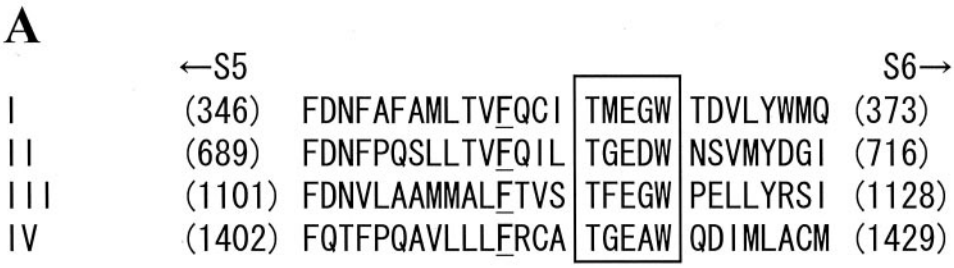

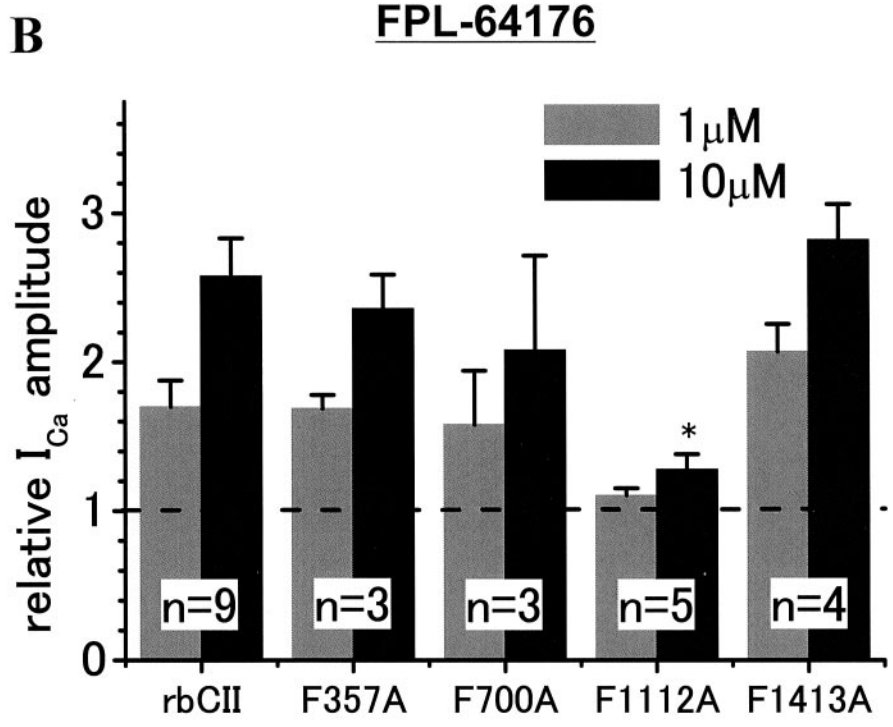

Fig. 3. Effects of FPL-64176 (1 μM) on Ca^{2+} channel currents through F→A mutants in repeat I~IV. A, sequence alignment of the pore-forming S5-S6 regions of rbCII. I~IV denote repeat I~IV. Phe mutated in this experiment are underlined. B, relative enhancement by FPL-64176 of peak Ca^{2+} channel currents through F357A, F700, F1112A, and F1413A. Only the mutation of Phe in IIIS5-S6 linker (F1112A) impaired the agonist action of FPL-64176. Horizontal dashed line indicates the control Ca^{2+} channel current level. *, $p < 0.01$ versus rbCII. Error bars show S.E.M.

Ca^{2+} channel agonists behaved as if they were weak Ca^{2+} channel antagonists in F1112A/S1115A. Then we compared effects on F1112A/S1115A of the stereoisomers (*S*)-(−)-Bay k 8644 and (*R*)-(+)-Bay k 8644, with the aim to further investigate the role of Phe^{1112}/Ser^{1115} in transducing the action of Ca^{2+} channel agonist and antagonist. Because ethanol used as solvent in DHP stock solution produces a Ca^{2+} channel blocking action at concentrations higher than 0.03% (Walter and Messing, 1999), Ca^{2+} channel current amplitudes were normalized to the control value measured in Tyrode's solution containing vehicle before the drug application. In rbCII, Ca^{2+} channel currents were enhanced by (*S*)-(−)-Bay k 8644 and blocked by (*R*)-(+)-Bay k 8644 at holding potentials of −70 and −50 mV (Fig. 8). At −50 mV, the enhancement of Ca^{2+} channel currents through rbCII by (*S*)-(−)-Bay k 8644 was smaller than that measured at −70 mV. In sharp contrast, Ca^{2+} channel currents through F1112A/S1115A were

TABLE 2

Relative potency of nitrendipine for the block of I_{Ca} recorded by giving test pulses to 0 mV for 100 ms from a holding potential at −70 mV at 0.1 Hz

	IC_{50}	Fold Increase vs. rbCII	*n*
	μM		
rbCII	0.504 ± 0.141		3
F1112A	2.58 ± 0.117	5.13	4
S1115A	19.9 ± 3.83*	39.4	3
F1112A/S1115A	25.3 ± 3.20*	50.2	4

* $P < 0.01$ versus rbCII.

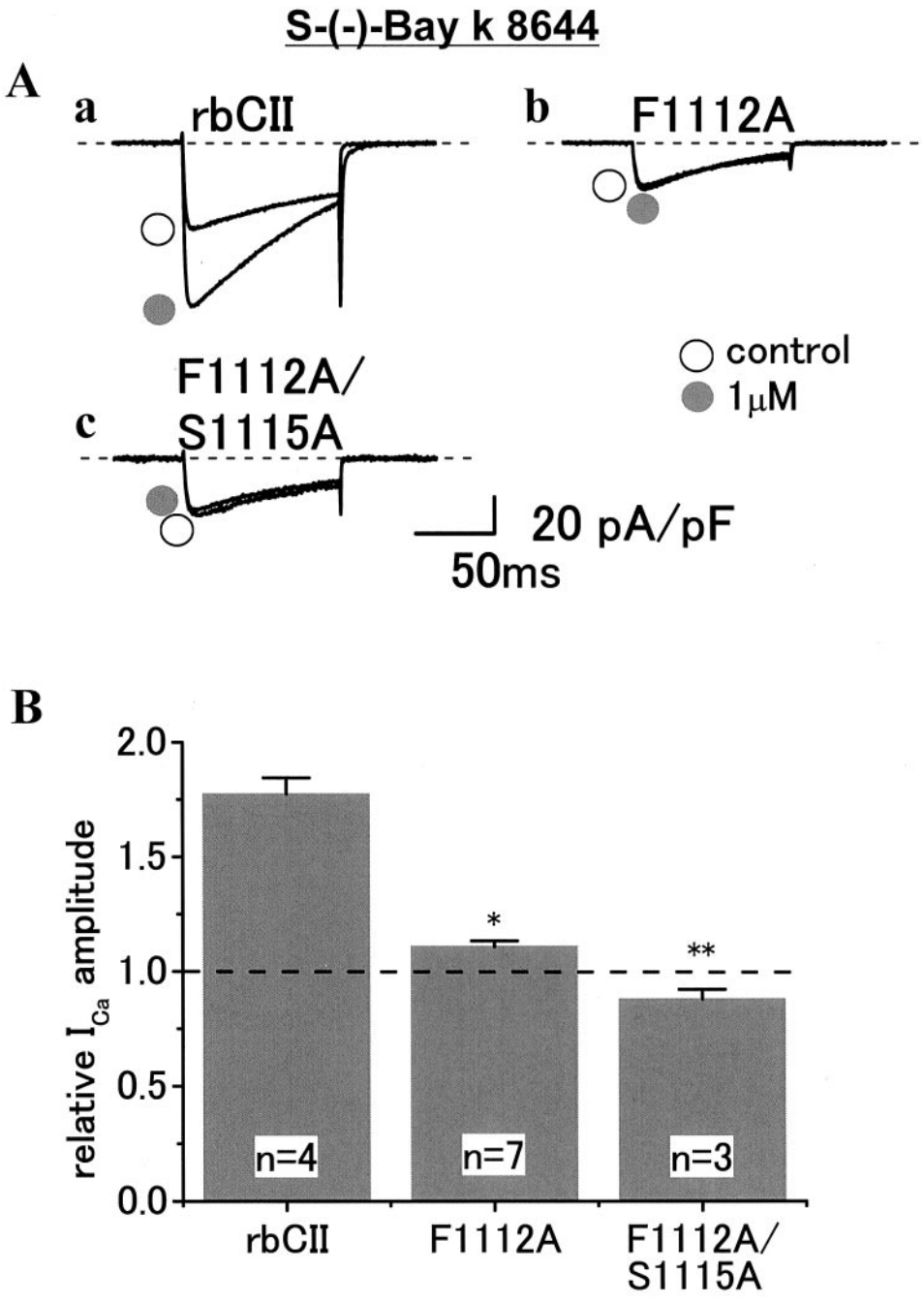

Fig. 4. Ca^{2+} agonists hardly enhanced Ca^{2+} channel currents through F1112A. A, representative current traces of rbCII (a), F1112A (b), and F1112A/S1115A (c) measured with and without (*S*)-(−)-Bay k 8644. Ca^{2+} channel currents were elicited by test pulses to 0 mV for 100 ms from a holding potential of −70 mV at 0.1Hz. Circles represent control (○) and Ca^{2+} channel currents measured in the presence of (*S*)-(−)-Bay k 8644 (1 μM) (◉). B, summary of relative enhancement of peak Ca^{2+} channel currents by (*S*)-(−)-Bay k 8644. Horizontal dashed line indicates control Ca^{2+} channel current level. *, $p < 0.05$ versus rbCII. **, $p < 0.01$ versus rbCII and $p < 0.05$ versus F1112A. Error bars show S.E.M.

slowly inhibited by agonist (*S*)-(−)-Bay k 8644 and recovered to the control level on washout (data not shown). (*R*)-(+)-Bay k 8644 also produced the block of Ca^{2+} channel currents to the same degree with the same time course and the voltage dependence as those of (*S*)-(−)-Bay k 8644. The blocking action of (*R*)-(+)-Bay k 8644 was significantly weaker in F1112A/S1115A compared with that of rbCII (Fig. 8), as was observed with nitrendipine (Table 2). These results indicate that F1112A/S1115A could not distinguish between the stereoisomers of Ca^{2+} agonist and antagonist.

Interestingly, FPL-64176 also behaved as an antagonist on F1112A/S1115A (Fig. 2B). Unitary currents through F1112A/S1115A were neither enhanced nor prolonged by FPL-64176 (Fig. 7C). These results indicate that F1112A/S1115A has completely lost the ability to be activated by Ca^{2+} channel agonists. In other words, Ca^{2+} channel agonists block F1112A/S1115A.

Importance of Aromatic Side Group of Phe^{1112} on the Action of Ca^{2+} Channel Agonists. We showed that the replacement of Phe^{1112} in IIIS5-S6 linker of Ca^{2+} channel by Ala reduced the binding affinity for DHPs and sensitivity to Ca^{2+} channel agonists. To elucidate the role of aromatic side group of Phe^{1112}, we introduced Tyr in place of Phe^{1112}. Effects of the mutation were evaluated by comparison of effects of FPL-64176 (Fig. 9A) on peak I_{Ca} (Fig. 9B) and the amount of Ca^{2+} entry through the Ca^{2+} channel ($\int I_{Ca}$) (Fig. 9C) between rbCII and mutant Ca^{2+} channels. The amount of Ca^{2+} entry through the Ca^{2+} channel, $\int I_{Ca}$, was estimated by integrating I_{Ca} during test potential. The increase of $\int I_{Ca}$ represents the prolongation of mean open time as well as the enhancement of open probability. Peak I_{Ca} and $\int I_{Ca}$ of rbCII were markedly enhanced by FPL-64176 in a concentration-dependent manner. The relative enhancement of $\int I_{Ca}$ was larger than that of peak amplitude of I_{Ca}. In contrast, in F1112A, peak I_{Ca} and $\int I_{Ca}$ were only slightly increased by FPL-64176 at 10 μM. Interestingly, the peak I_{Ca} through F1112Y was slightly enhanced by FPL-64176 to the extent similar to that of F1112A (Fig. 9B), but the increment of $\int I_{Ca}$ was significantly larger than that of F1112A (Fig. 9C). The enhancement of peak I_{Ca} of rbCII by FPL-64176 at 1 μM was almost equivalent to the enhancement of F1112Y and F1112A by FPL-64176 at 10 μM. However, when the three bar graphs were compared (rbCII with FPL-64176 at 1 μM, F1112Y with 10 μM, and F1112A with 10 μM), the enhancement of $\int I_{Ca}$ was significantly larger in rbCII and F1112Y than in F1112A. These results were consistent with results of single-channel experiments, where the prolongation of the mean open time by FPL-64176 was significantly larger in rbCII and F1112Y than in F1112A (Fig. 7). On the other hand, the increment of peak amplitude of I_{Ca} and $\int I_{Ca}$ was smaller in F1112Y than in rbCII, thus indicating that the replacement of Phe^{1112} by Tyr had reduced the sensitivity to

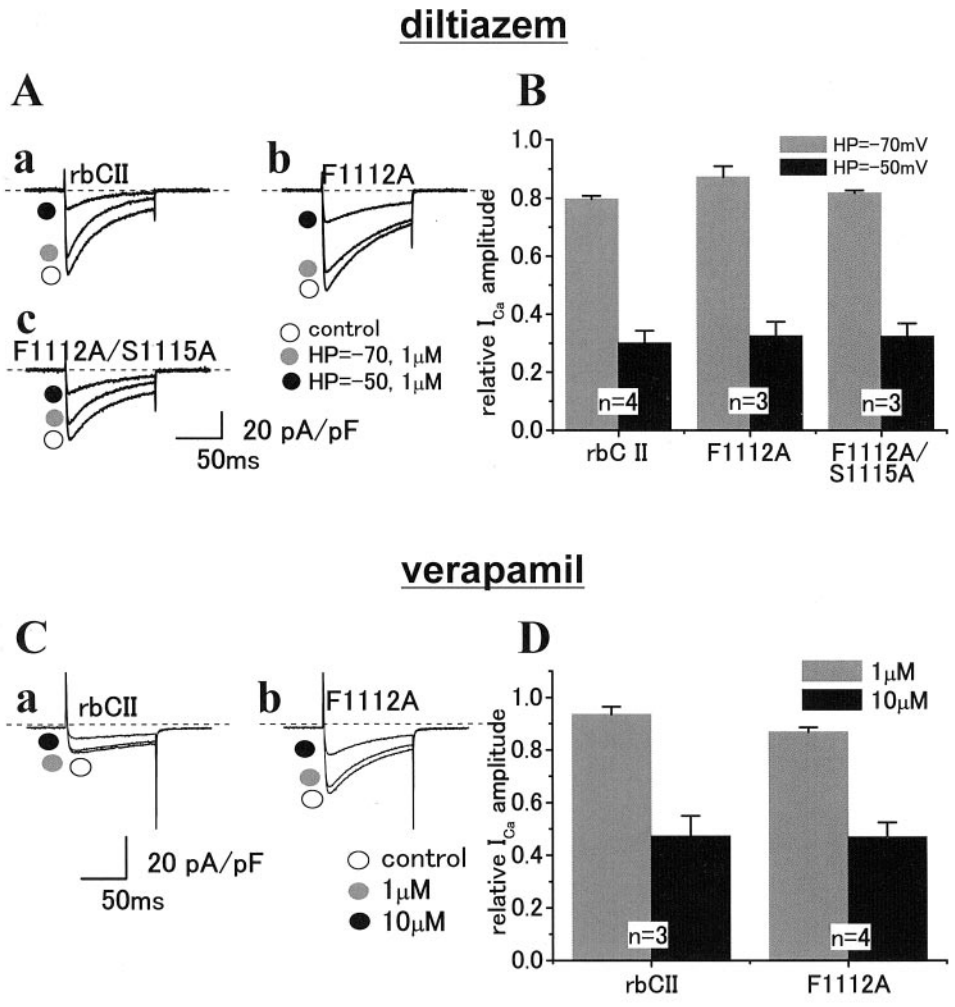

Fig. 5. The inhibition of Ca^{2+} channel currents by diltiazem (1 μM) or verapamil (1, 10 μM) was not different between rbCII and mutant Ca^{2+} channels. A, representative current traces of rbCII (a), F1112A (b), and F1112A/S1115A (c) with and without diltiazem. Ca^{2+} channel currents were elicited by test pulses to 0 mV for 100 ms from a holding potential of −70 mV applied at 0.1 Hz. ○, control Ca^{2+} channel currents recorded at a holding potential of −70 mV. Other circles represent Ca^{2+} channel currents measured in the presence of diltiazem (1 μM) at holding potentials of −70 mV (◍) and −50 mV (●). B, relative Ca^{2+} channel current amplitudes measured in the presence of diltiazem (1 μM) at holding potentials of −70 and −50 mV. There were no significant differences between rbCII and mutant Ca^{2+} channels. C, representative current traces of rbCII (a) and F1112A (b). Ca^{2+} channel currents were elicited by test pulses to 0 mV applied at 0.2Hz. ○, control Ca^{2+} channel currents. Other circles represent Ca^{2+} channel currents inhibited by 1 mM (◍) or 10 μM (●) verapamil. D, relative Ca^{2+} channel current amplitudes measured in the presence of verapamil (1 and 10 μM). There were no significant differences between rbCII and F1112A. The error bars show S.E.M.

Ca^{2+} channel agonists. Nevertheless, these results suggest that the aromatic ring of Phe^{1112} plays a critical role in the prolongation of the open time produced by FPL-64176.

Modeling DHP-rbCII Binding. In a three-dimensional model, orientation of residues depends dramatically on the alignment between KcsA and rbCII. The alignment shown in Table 1 yields a model in which several residues whose mutation affects DHP binding (DHP-sensing residues) form a ligand-binding pocket in the interface between repeats III and IV (interface III/IV). A DHP ligand bound in this pocket is partially exposed to the central pore (Fig. 3B in Zhorov et al., 2001). To assess whether residues in the IIIS5-S6 linker can contribute to the ligand binding, a typical DHP antagonist, nifedipine, was docked from a hundred of randomly generated starting positions and orientations, the center of distribution being in the III/IV interface. During each docking, the energy was Monte Carlo-minimization as described previously (Zhorov et al., 2001).

Forty lowest-energy structures collected from these trajectories show that nifedipine can populate large areas in the central pore, in the III/IV interface, and between the pore and the III/IV interface (Fig. 10A). Interestingly, flexible DHP-sensing residues $Tyr^{IIIS6.10}$, $Met^{IIIS6.18}$, $Tyr^{IVS6.11}$, and $Met^{IVS6.12}$ can interact with nifedipine bound in the pore and in the III/IV interface. According to calculations, nifedipine binding in the pore is energetically preferable. It should be noted, however, that the current model does not include segments S1 to S4, some of which could enhance DHP binding in the III/IV interface.

Figure 10B shows possible ligand-binding pockets in the III/IV interface formed by 10 DHP-sensing residues: $Ser^{1115(IIIP.47)}$, $Phe^{1112(IIIP.44)}$, $Thr^{IIIS5.14}$, $Gln^{IIIS5.18}$, $Tyr^{IIIS6.10}$, $Ile^{IIIS6.14}$, $Met^{IIIS6.18}$, $Tyr^{IVS6.11}$, $Met^{IVS6.12}$, and $Ile^{IVS6.19}$. Calculations predict several essentially different orientations of nifedipine in this pocket. No experimental data are currently available to favor one of the orientations. DHP-sensing residues $Ile^{IIIS6.11}$, $Met^{IIIS6.19}$, $Ile^{IVS6.18}$, and $Asn^{IVS6.20}$, as well as Ca^{2+} ion coordinated by the selectivity-filter glutamates, do not contribute to the DHP-binding in the III/IV interface. Some DHP-sensing residues are too far from each other and cannot bind simultaneously to a ligand. For example, the distance between C^{β}_$Phe^{IIIP.44}$ and C^{β}_$Ile^{IVS6.19}$ (18.3 Å) is significantly larger than the maximal possible distance between nifedipine atoms (11.4 Å) (Zhorov and Ananthanarayanan, 1996).

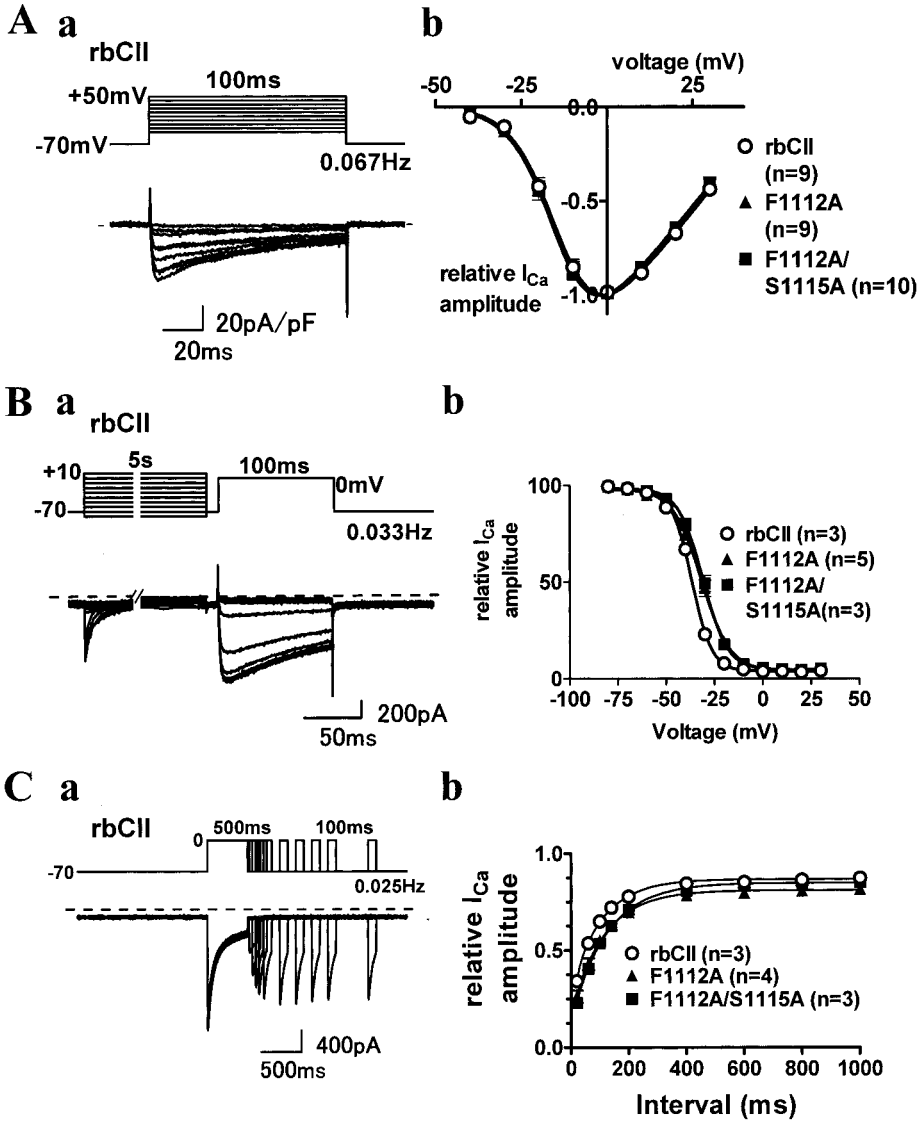

Fig. 6. Electrophysiological properties of F1112A and F1112A/S1115A. A, current-voltage relationships of rbCII (○, $n = 9$), F1112A (▲, $n = 9$), and F1112A/S1115A (■, $n = 10$) are superimposed. Charge carrier was Ca^{2+} (2 mM). Currents were normalized to the peak current amplitude evoked by test pulses to 0 mV. There were no significant differences in peak Ca^{2+} channel current density between rbCII and F1112A/S1115A (rbCII, -43.1 ± 5.1 pA/pF ($n = 9$); F1112A/S1115A, -54.3 ± 5.6 pA/pF ($n = 10$)). B, steady-state inactivation curve of rbCII (○, $n = 3$), F1112A (▲, $n = 5$), and F1112A/S1115A (■, $n = 3$) were measured with voltage protocol shown in B, a. Charge carrier was Ba^{2+} (2 mM). Representative current traces of rbCII are shown in B, a. Pulses were applied every 30 s.

Discussion

Alanine-Scanning Mutagenesis of IIIS5-S6-Linker. In this study, we present a novel insight into the molecular mechanism underlying modulation of gating kinetics of L-type Ca^{2+} channels by DHP and non-DHP Ca^{2+} channel agonists. By use of alanine-scanning mutagenesis, we identified amino acid residue $Phe^{1112(IIIP44)}$, in addition to $Ser^{1115(IIIP47)}$, as an important determinant of DHP binding and action of Ca^{2+} channel agonist (Fig. 2). The requirement of $Phe^{1112(IIIP44)}$ as well as $Ser^{1115(IIIP47)}$ in the IIIS5-S6 linker for the action of Ca^{2+} channel agonists highlights the important role of the pore helix in the modulation of the gating kinetics by Ca^{2+} channel agonists.

Contrary to F1112A, the sensitivity of T1113A to Ca^{2+} channel agonists was enhanced (Fig. 2), although T1113A channel was inhibited by DHP antagonist in a manner similar to that of rbCII (data not shown). The substitution of $Thr^{1113(IIIP45)}$ by Ala may have turned the side chain of adjacent $Phe^{1112(IIIP44)}$ to the favorable arrangement for

TABLE 3
Equilibrium binding of [^{3}H] PN200–110 to mutant Ca^{2+} channels.

	K_d	Fold Increase vs rbCII	B_{max}	n
	nM		*fmol/mg protein*	
rbCII	0.14 ± 0.017		488 ± 55.5	6
F1112A	0.84 ± 0.203	6	288 ± 37.3	4
S1115A	* 23.5 ± 7.28	165	562 ± 134	4

* $P < 0.01$ versus rbCII

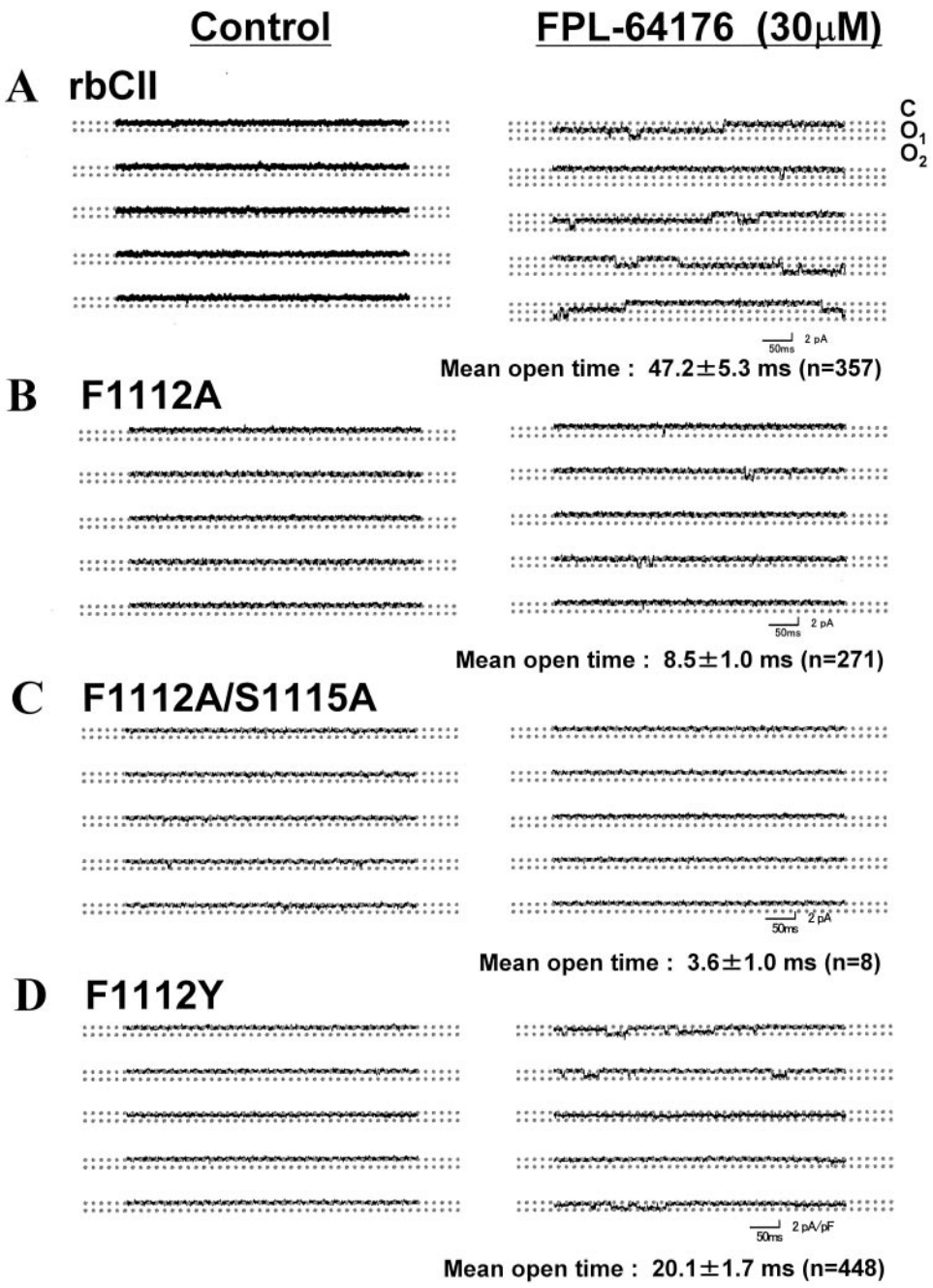

Fig. 7. Effects of FPL-64176 on unitary Ca^{2+}channel currents. Single channel recording of rbCII (A), F1112A(B), F1112A/S1115A (C), and F1112Y (D) before (left) and after (right) application of FPL-64176 (30 μM). Holding potential was −60 mV and test potential was −10 mV. The open probabilities of unitary currents through F1112A and F1112A/S1115A were not enhanced by Ca^{2+} channel agonists, and long opening states were not observed.

Ca^{2+} channel agonists to exert their action or may have reduced the steric hindrance for the access of Ca^{2+} channel agonists.

Is the insensitivity of $Phe^{1112(IIIP44)}$ (and $Ser^{1115(IIIP47)}$) to Ca^{2+} channel agonists attributed to the reduction of the binding affinity? To answer this question, we compared the sensitivity and the binding affinity of mutant Ca^{2+} channels to DHP antagonists. As summarized in Tables 2 and 3, the relative differences of sensitivity and binding affinity to DHP antagonists between rbCII and F1112A were comparable. From the comparison between two independent experiments, we concluded that the low sensitivity of Ca^{2+} channel currents of F1112A or S1115A to DHP antagonists is compatible with the reduced binding affinity to them. From these experiments, it could be anticipated that the binding affinity of F1112A or S1115A for DHP agonists was decreased to the same extent as that for DHP antagonists and that the insensitiveness to DHP agonists could have been caused by the reduction of binding affinity.

The prolongation of open time by FPL-64176, assessed by $\int I_{Ca}$ and mean open time (Figs. 7 and 9C), was retained in rbCII and F1112Y but was mostly absent in F1112A, thus indicating that the aromatic side chain of $Phe^{1112(IIIP44)}$ is required for producing full agonistic effects by FPL-64176. If this functional group is missing, Ca^{2+} agonists may not be able to stabilize the open states.

Synergistic Effects of $Phe^{1112(IIIP44)}$ and $Ser^{1115(IIIP47)}$ to the Action of DHPs. If $Phe^{1112(IIIP44)}$ (or $Ser^{1115(IIIP47)}$) simply serves as a binding pocket for DHP,

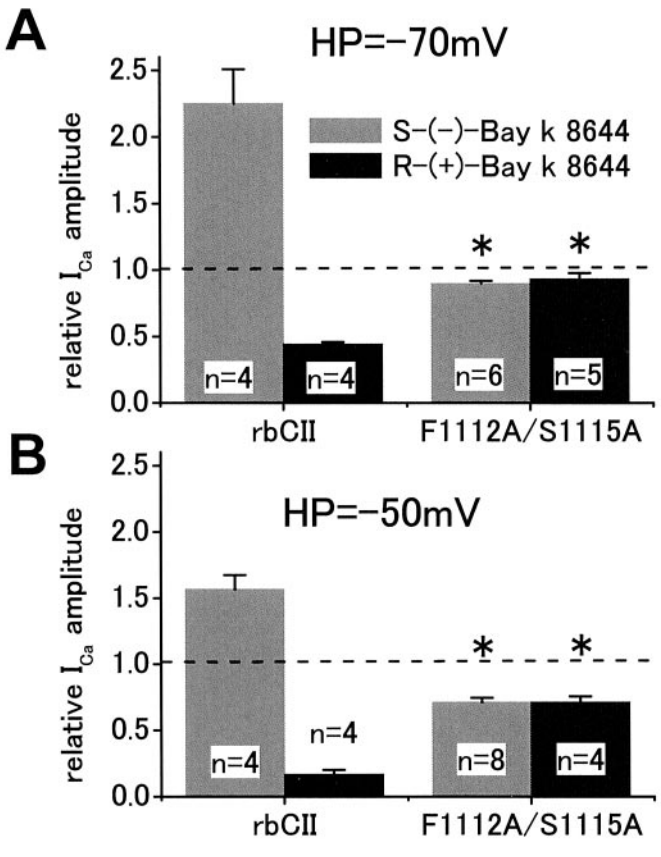

Fig. 8. Block of F1112A/S1115A channel by stereoisomers, (*S*)-(−)-Bay k 8644 and (*R*)-(+)-Bay k 8644. The voltage-dependent inhibition of peak Ca^{2+} channel currents by (*S*)-(−)-Bay k 8644 (10 μM) and (*R*)-(+)-Bay K 8644 (10 μM) is summarized. (*S*)-(−)-Bay k 8644, a DHP agonist, enhanced Ca^{2+} channel currents through rbCII but inhibited that of F1112A/S1115A at holding potentials of −50 and −70 mV. Effects of (*R*)-(+)-Bay k 8644, a DHP antagonist, on Ca^{2+} channel currents through F1112A/S1115A were weaker than that of rbCII. Consequently, (*S*)-(−)-Bay k 8644 and (*R*)-(+)-Bay k 8644 showed equal inhibition of F1112A/S1115A channel. *, $p < 0.005$ versus rbCII. The error bars show S.E.M.

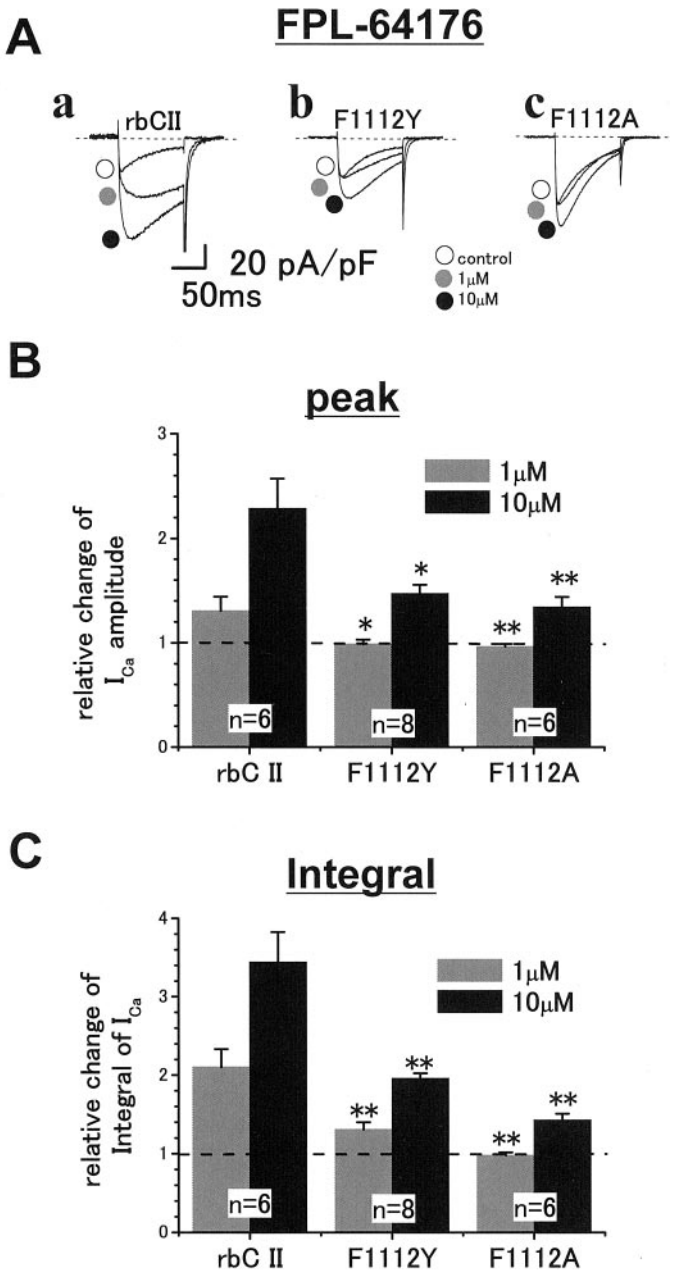

Fig. 9. Effects of substitution of Tyr for $Phe^{1112(IIIP44)}$. A, representative current traces of rbCII (a), F1112Y (b), and F1112A (c) measured with and without FPL-64176 (1 and 10 μM). Ca^{2+} channel currents were elicited by test pulses to 0 mV for 100 ms from a holding potential of −70 mV at 0.1Hz. ○, control Ca^{2+} channel currents. Other circles represent Ca^{2+} channel currents recorded in the presence of FPL-64176 at 1 μM (◍) and 10 μM (●). B, summary of relative enhancement of peak Ca^{2+} channel currents by FPL-64176. Horizontal dashed line indicates control Ca^{2+} channel current level recorded in the bath solution including vehicle (0.03% ethanol). *, $p < 0.05$ versus rbCII. **, $p < 0.01$ versus rbCII. C, summary of relative enhancement of total amount of Ca^{2+} entry through Ca^{2+} channel by FPL-64176. Horizontal dashed line indicates integral of Ca^{2+} channel current without FPL-64176. *, $p < 0.05$ versus rbCII. **, $p < 0.01$ versus rbCII. Error bars show S.E.M.

Ca^{2+} currents through the double-mutant Ca^{2+} channel F1112A/S1115A would be slightly enhanced (although weaker than through the single-mutant channels) or would be unaffected by Ca^{2+} agonists. However, effects of Ca^{2+} agonists on F1112A/S1115A were quite distinctive. Unexpectedly, Ca^{2+} agonists decreased rather than increased Ca^{2+} currents through F1112A/S1115A (Figs. 2, 4, and 8). The weak blocking action of the Ca^{2+} channel agonists on F1112A/S1115A conceivably reflects the interaction between Ca^{2+} agonists and F1112A/S1115A, even though the binding affinity may be somewhat lower. Furthermore, the single channel currents through F1112A/S1115A were not prolonged at all by FPL-64176 (Fig. 7). It is likely that, in F1112A/S1115A, the interaction with Ca^{2+} agonists is not transmitted to the Ca^{2+} channel agonistic action. Importantly, in the double mutant F1112A/S1115A, Ca^{2+} agonists behaved as if they were weak Ca^{2+} antagonists. Furthermore, F1112A/S1115A was not able to distinguish between (*S*)-(−)-Bay k 8644 and (*R*)-(+)-Bay k 8644. Thus, the two amino acid residues seem to serve as a decisive factor for agonist/antagonist actions of Ca^{2+} channel modulators. We propose that $Phe^{1112(IIIP44)}$ and $Ser^{1115(IIIP47)}$ have two functions: 1) they are part of a binding pocket for DHPs and 2) they are the key residues for transducing the binding of Ca^{2+} channel agonists into the agonistic action, such as stabilization of Ca^{2+} channels in the open state.

Under certain conditions (e.g., at very high concentrations or at depolarizing voltages), DHP agonists exert antagonistic effects (Adachi-Akahane and Nagao, 2000). Thus, the conformational state of the α_{1C} subunit seems to be a major factor in determining the agonist/antagonistic action of DHPs (Triggle and Rampe, 1989). In the present study, we demonstrated that substitution of $Phe^{1112(IIIP44)}$ and $Ser^{1115(IIIP47)}$ with Ala results in Ca^{2+} channel agonists exhibiting effects of weak antagonists. Therefore, in the wild-type channel, the interaction of Ca^{2+} agonists with $Phe^{1112(IIIP44)}$ and $Ser^{1115(IIIP47)}$ may be disrupted at the depolarized voltages.

Contribution of $Phe^{1112(IIIP44)}$ and $Ser^{1115(IIIP47)}$ to the DHP-Binding Pocket. Most of the binding sites for Ca^{2+} channel agonists and antagonists have been determined by comparison between α_{1C} and α_{1A} sequences. Therefore, the amino acids highly conserved between DHP- and non–DHP-sensitive Ca^{2+} channel α_1 subunits have been excluded. However, some amino acid residues common between α_{1C} and α_{1A} have been identified as critical binding sites (Bodi et al., 1997; Peterson et al., 1997; Wappl et al., 2001). In fact, $Phe^{1112(IIIP44)}$ and $Ser^{1115(IIIP47)}$ are conserved in high-voltage activated Ca^{2+} channels. Phe residues in position P44 are highly conserved in the P regions of voltage-dependent Ca^{2+} and Na^+ channels. However, Phe^{IP44}, Phe^{IIP44}, and Phe^{IVP44} seem unrelated to Ca^{2+} channel agonist action (Fig. 3).

Mutation of Phe^{IIIP49} preceding the selectivity-filter Glu^{IIIP50} reportedly affects the DHP binding (Peterson and Catterall, 1995). In this study, Phe^{IIIP49} was excluded from targets for alanine-scanning mutagenesis (see *Results*).

DHP Binding Model. Earlier mutational studies revealed DHP-sensing residues in segments IIIS5, IIIS6, and IVS6 (Table 1). In addition, Ca^{2+} coordination by the selectivity-filter glutamates is important for DHP binding (Mitterdorfer et al., 1995; Peterson and Catterall, 1995). Present study indicates that mutations of $Ser^{1115(IIIP47)}$ and $Phe^{1112(IIIP.44)}$ also affect DHP binding.

The X-ray structure of a bacterial K^+ channel KcsA was used as a template to build homology models of L-type Ca^{2+} channel that visualize DHPs bound in the III/IV interface

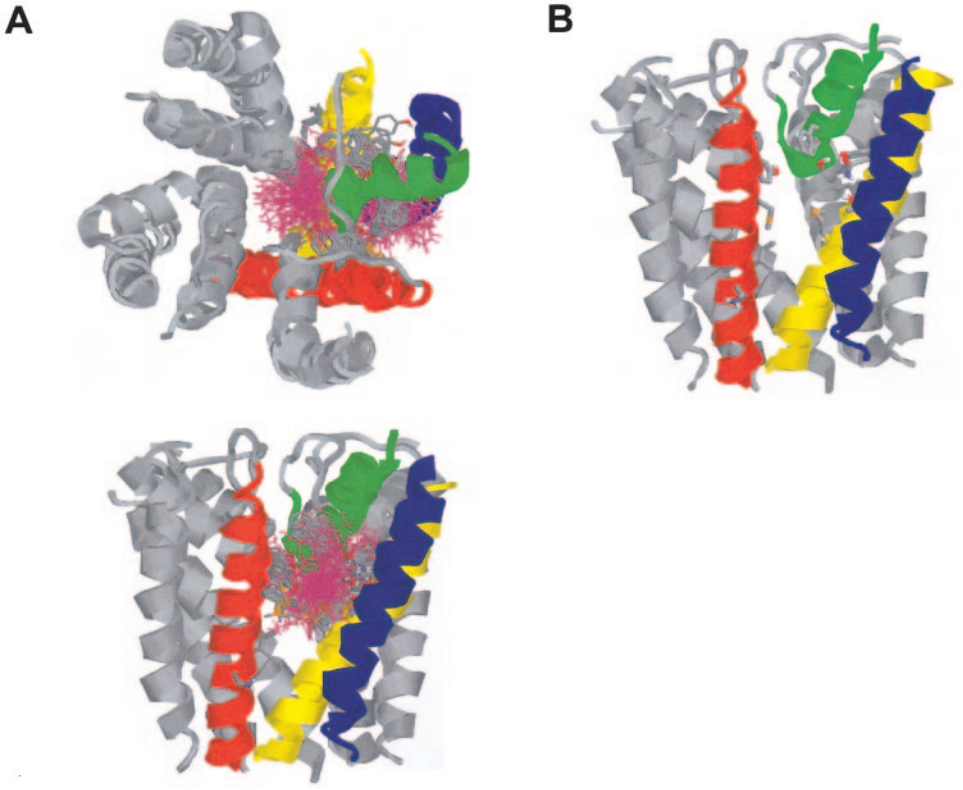

Fig. 10. A, top and side views at the superposition of 40 Monte Carlo-minimized complexes of the rbCII model with nifedipine. Segments IIIS5, IIIS6, IVS6, and the N-terminal part of IIIP are shown as yellow, blue, red, and green helices, respectively. DHP-sensing residues are shown by thick sticks. Nifedipine is shown by thin magenta sticks. Note that long side chains of $Tyr^{IIIS6.10}$, $Tyr^{IVS6.11}$, and several other DHP-sensing residues can interact with the DHP ligand in the central pore as well as in interface III/IV. B, interface III/IV of rbCII viewed from outside of the channel. DHP-sensing residues $Ser^{1115(IIIP.47)}$, $Phe^{1112(IIIP.44)}$, $Thr^{IIIS5.14}$, $Gln^{IIIS5.18}$, $Tyr^{IIIS6.10}$, $Ile^{IIIS6.14}$, $Met^{IIIS6.18}$, $Tyr^{IVS6.11}$, $Met^{IVS6.12}$, $Ile^{IVS6.19}$, and $Asn^{IVS6.20}$ are shown by thick sticks. Clear space between IIIS6 and IVS6 would allow the ligand to move between the III/IV interface and the central pore.

(Huber et al., 2000) and in the pore (Zhorov et al., 2001). Finding of DHP-sensing residues in the pore helix of segment IIIP provides additional constraints for modeling the DHP-binding site(s). The alignment shown in Table 1 yields a model in which $Ser^{1115(IIIP47)}$, $Phe^{1112(IIIP.44)}$, and several other DHP-sensing residues can contribute to DHP binding in the III/IV interface.

DHP agonists and antagonists were suggested to exert their effect from the pore-binding site (Zhorov et al., 2001). Mutational and modeling data of the present study do not rule out this possibility but suggest that the III/IV interface site is also important. Interestingly, several DHP-sensing residues, including $Tyr^{IIIS6.10}$ and $Tyr^{IVS6.11}$, critical determinants of DHP binding, can interact with DHP ligand in the III/IV interface as well as in the pore (Fig. 10A).

The fact that double mutant F1112A/S1115A is blocked rather than activated by agonist (*S*)-(−)-Bay k 8644 seems inconsistent with the idea that the agonist binds inside the pore. One possibility to resolve this conflict is to suggest that DHPs bind in the III/IV interface on their way from the extracellular space to the pore. In the energetically preferable conformation, the DHP ring has a flattened-boat form. Enantiomers of Bay k 8644 have different substituents at the port side of the boat: the agonist has a hydrophilic NO_2 group, whereas antagonist has a hydrophobic COOMe group. The effect of a DHP ligand would depend on how it approaches the hydrophobic gate at the S6 crossing: if near the hydrophobic group, it would act as the antagonist; if by the hydrophilic group, it would act as the agonist (Zhorov et al., 2001). Once inside the channel, the bulky DHP ligand cannot flip-flop. If the DHP agonist (*S*)-(−)-Bay k 8644 enters the III/IV interface by the port-side hydrophilic group forward, it would approach the gate by this group and would act as the agonist. If the agonist enters the interface with the starboard hydrophobic group forward, it would approach the gate by this group and would act as the antagonist. According to calculations, the port-side–down and starboard-side–down orientations of a DHP ligand in the pore are almost equal in energy (Zhorov et al., 2001). In the wild-type channel, $Phe^{1112(IIIP44)}$ and $Ser^{1115(IIIP47)}$ may stabilize the port-side–down orientation of the Bay k 8644 enantiomers in the III/IV interface, thus predetermining the ligand orientation in the pore and hence the type of its activity. The double mutant would not stabilize the port-side–down orientation of the ligand in the III/IV interface. The agonist (*S*)-(−)-Bay k 8644 would enter the interface by its starboard hydrophobic group forward simply because $Ala^{1112(IIIP44)}$ and $Ala^{1115(IIIP47)}$ in the double mutant make a more hydrophobic entrance than $Phe^{1112(IIIP44)}$ and $Ser^{1115(IIIP47)}$ in the wild-type channel. As the result, the agonist would approach the S6 crossing by the hydrophobic starboard group and would act as the antagonist.

Thus, the KcsA-based model of rbCII cannot visualize all known DHP-sensing residues in direct contacts with a DHP molecule. This suggests two possibilities: 1) mutations of some DHP-sending residues affect ligand binding indirectly, and 2) the effect of DHPs on the channel gating depends on their binding to more than one site in the pore-forming subunit. Further experimental and theoretical studies are necessary to explore these possibilities.

In conclusion, the present study postulates two possibilities for the selective loss of sensitivity to Ca^{2+} channel agonists and DHPs: 1) $Phe^{1112(IIIP44)}$ and $Ser^{1115(IIIP47)}$ are binding sites for DHPs or 2) $Phe^{1112(IIIP44)}$ and $Ser^{1115(IIIP47)}$ are required for the transmission of the drug binding into its action as Ca^{2+} channel agonists (Fig. 10). Elucidation of the role of $Phe^{1112(IIIP44)}$ and $Ser^{1115(IIIP47)}$ in the modulation of Ca^{2+} channel gating by Ca^{2+} channel agonists would be helpful for understanding the role of the pore-forming region in the modulation of Ca^{2+} channel gating by Ca^{2+} channel modulators and refining the three-dimensional structure model of the pore-forming region of L-type Ca^{2+} channel α_{1C} subunit.

Acknowledgments

We are grateful to Dr. T. P. Snutch for generous gift of rbCII and Dr. Y. Mori for BHK6 cells. We thank Tanabe Seiyaku Co. Ltd. for generous supply of *d-cis*-diltiazem.

References

Adachi-Akahane S, Cleemann L, and Morad M (1996) Cross-signaling between L-type Ca^{2+} channels and ryanodine receptors in rat ventricular myocytes. *J Gen Physiol* **108:**435–454.

Adachi-Akahane S and Nagao T (2000) Ca^{2+} channel antagonists and agonists, in *Pharmacology of Ionic Channel Function: Activators and Inhibitors* (Endo M, Kurachi Y, Mishina M eds) Handbook of Experimental Pharmacology, Vol. 147, pp 119–154, Springer, New York.

Bean BP (1984) Nitrendipine block of cardiac calcium channels - high-affinity binding to the inactivated state. *Proc Natl Acad Sci USA* **81:**6388–6392.

Blaber M, Zhang XJ, and Matthews BW (1993) Structural basis of amino-acid alpha-helix propensity blabber. *Science (Wash DC)* **260:**1637–1640.

Bodi I, Yamaguchi H, Hara M, He M, Schwartz A, and Varadi G (1997) Molecular studies on the voltage dependence of dihydropyridine action on L-type Ca^{2+} channels—critical involvement of tyrosine residues in motif IIIS6 and IVS6. *J Biol Chem* **272:**24952–24960.

Doyle DA, Cabral JM, Pfuetzner RA, Kuo A, Gulbis JM, Cohen SL, Chait BT, and MacKinnon R (1998) The structure of the potassium channel: molecular basis of K^+ conduction and selectivity. *Science (Wash DC)* **280:**69–77.

Glossmann H and Striessnig J (1990) Molecular-properties of calcium channels. *Rev Physiol Biochem Pharmacol* **114:**1–105.

Grabner M, Wang ZY, Hering S, Striessnig J, and Glossmann H (1996) Transfer of 1,4-dihydropyridine sensitivity from L-type to class A (BI) calcium channels. *Neuron* **16:**207–218.

He M, Bodi I, Mikala G, and Schwartz A (1997) Motif III S5 of L-type calcium channels is involved in the dihydropyridine binding site. A combined radioligand binding and electrophysiological study. *J Biol Chem* **272:**2629–2633.

Hockerman GH, Peterson BZ, Sharp E, Tanada TN, Scheuer T, and Catterall WA (1997) Construction of a high-affinity receptor site for dihydropyridine agonists and antagonists by single amino acid substitutions in a non–L-type Ca^{2+} channel. *Proc Natl Acad Sci USA* **94:**14906–14911.

Huber I, Wappl E, Herzog A, Mitterdorfer J, Glossmann H, Langer T, and Striessnig J (2000) Conserved Ca^{2+}-antagonist-binding properties and putative folding structure of a recombinant high-affinity dihydropyridine-binding domain. *Biochem J* **347:**829–836.

Ikeda S, Amano Y, Adachi-Akahane S, and Nagao T (1994) Binding of [^{3}H](+)-PN200-110 to aortic membranes from normotensive and spontaneously hypertensive rats. *Eur J Pharmacol* **264:**223–226.

Kunze DL and Rampe D (1992) Characterization of the effects of a new Ca^{2+} channel activator, FPL-64176, in GH3 cells. *Mol Pharmacol* **42:**666–670.

Lipkind GM and Fozzard HA (2001) Modeling of the outer vestibule and selectivity filter of the L-type Ca^{2+} channel. *Biochemistry* **40:**6786–6794.

Mitterdorfer J, Sinnegger MJ, Grabner M, Striessnig J, and Glossmann H (1995) Coordination of Ca^{2+} by the pore region glutamates is essential for high-affinity dihydropyridine binding to the cardiac Ca^{2+} channel α_1 Subunit**.** *Biochemistry* **34:**9350–9355.

Mitterdorfer J, Wang Z, Sinnegger MJ, Hering S, Striessnig J, Grabner M, and Glossmann H (1996) Two amino acid residues in the IIIS5 segment of L-type calcium channels differentially contribute to 1,4-dihydropyridine sensitivity. *J Biol Chem* **271:**30330–30335.

Peterson BZ and Catterall WA (1995) Calcium-binding in the pore of L-type calcium channels modulates high-affinity dihydropyridine binding. *J Biol Chem* **270:**18201–18204.

Peterson BZ, Johnson BD, Hockerman GH, Acheson M, Scheuer T, and Catterall WA (1997) Analysis of the dihydropyridine receptor site of L-type calcium channels by alanine-scanning mutagenesis. *J Biol Chem* **272:**18752–18758.

Peterson BZ, Tanada TN, and Catterall WA (1996) Molecular determinants of high affinity dihydropyridine binding in L-type calcium channels. *J Biol Chem* **271:**5293–5296.

Rampe D and Lacerda AE (1991) A new site for the activation of cardiac calcium channels defined by the nondihydropyridine FPL-64176. *J Pharmacol Exp Ther* **259:**982–987.

Regulla S, Schneider T, Nastainczyk W, Meyer HE, and Hofmann F (1991) Identification of the site of interaction of the dihydropyridine channel blockers nitren-

dipine and azidopine with the calcium-channel α_1 subunit. *EMBO (Eur Mol Biol Organ) J* **10:**45–49.
Schuster A, Lacinová L, Klugbauer N, Ito H, Birnbaumer L, and Hofmann F (1996) The IVS6 segment of the L-type calcium channel is critical for the action of dihydropyridines and phenylalkylamines. *EMBO (Eur Mol Biol Organ) J* **15:**2365–2370.
Sinnegger MJ, Wang Z, Grabner M, Hering S, Striessnig J, Glossmann H, and Mitterdorfer J (1997) Nine L-type amino acid residues confer full 1, 4-dihydropyridine sensitivity to the neuronal calcium channel α_{1A} subunit. Role of L-type MET^{1188}. *J Biol Chem* **272:**27686–27693.
Snutch TP, Tomlinson WJ, Leonard JP, and Gilbert MM (1991) Distinct calcium channels are generated by alternative splicing and are differentially expressed in the mammalian CNS. *Neuron* **7:**45–57.
Striessnig J, Murphy BJ, and Catterall WA (1991) Dihydropyridine receptor of L-type Ca^{2+} channels: Identification of binding domains for [^{3}H](+)-PN200-110 and [^{3}H]azidopin within the α_1 subunit. *Proc Natl Acad Sci USA* **88:**10769–10773.
Striessnig J, Grabner M, Mitterdorfer J, Hering S, Sinnegger MJ, and Glossmann H (1998) Structural basis of drug binding to L Ca^{2+} channels. *Trends Pharmacol Sci* **19:**108–115.
Tang SQ, Mikala G, Bahinski A, Yatani A, Varadi G, and Schwartz A (1993) Molecular localization of ion selectivity sites within the pore of a human L-type cardiac calcium-channel. *J Biol Chem* **268:**13026–13029.
Triggle DJ and Rampe D (1989) 1,4-Dihydropyridine activators and antagonists: structural and functional distinctions. *Trends Pharmacol Sci* **10:**507–511.
Usowicz MM, Gigg M, Jones LME, Cheung CW, and Hartley SA (1995) Allosteric interactions at L-type calcium channels between FPL-64176 and the enantiomers of the dihydropyridine Bay k 8644. *J Pharmacol Exp Ther* **275:**638–645.
Wakamori M, Yamazaki K, Matsunodaira H, Teramoto T, Tanaka I, Niidome T, Sawada K, Nishizawa Y, Sekiguchi N, Mori E, et al. (1998) Single tottering mutations responsible for the neuropathic phenotype of the P-type calcium channel. *J Biol Chem* **273:**34857–34867.
Walter HJ and Messing RO (1999) Regulation of neuronal voltage-gated calcium channels by ethanol. *Neurochem Int* **35:**95–101.
Wappl E, Mitterdorfer J, Glossmann H, and Striessnig J (2001) Mechanism of dihydropyridine interaction with critical binding residues of L-type Ca^{2+} channel α_1 subunits. *J Biol Chem* **276:**12730–12735.
Williamson AV and Sather WA (1999) Nonglutamate pore residues in ion selection and conduction in voltage-gated Ca^{2+} channels. *Biophys J* **77:**2575–2589.
Yamaguchi S, Okamura Y, Nagao T, and Adachi-Akahane S (2000) Serine residue in the IIIS5–S6 linker of the L-type Ca^{2+} channel α_{1C} subunit is the critical determinant of the action of dihydropyridine Ca^{2+} channel agonists. *J Biol Chem* **275:**41504–41511.
Zheng W, Rampe D, and Triggle DJ (1991) Pharmacological, radioligand binding and electrophysiological characteristics of FPL-64176, a novel nondihydropyridine Ca^{2+} -channel activator, in cardiac and vascular preparations. *Mol Pharmacol* **40:**734–741.
Zhorov BS and Ananthanarayanan VS (1996) Structural model of a synthetic Ca^{2+} channel with bound Ca^{2+} ions and dihydropyridine ligand. *Biophys J* **70:**22–37.
Zhorov BS, Folkman EV, and Ananthanarayanan VS (2001) Homology model of dihydropyridine receptor: implications for L-type Ca^{2+} channel modulation by agonists and antagonists. *Arch Biochem Biophys* **393:**22–41.

Address correspondence to: Dr. Satomi Adachi-Akahane, Laboratory of Cell Signaling, Graduate school of Pharmaceutical Sciences, The University of Tokyo, 7-3-1 Hongo, Bunkyo-ku, Tokyo 113-0033, Japan. E-mail: satomiaa@mol.f.u-tokyo.ac.jp